Autoimmune arthritis associated with mutated interleukin (IL)-6 receptor gp130 is driven by STAT3/IL-7–dependent homeostatic proliferation of CD4$^+$ T cells

Shin-ichiro Sawa,[1] Daisuke Kamimura,[1,2] Gui-Hua Jin,[1] Hideyuki Morikawa,[1] Hokuto Kamon,[1] Mika Nishihara,[1] Katsuhiko Ishihara,[1] Masaaki Murakami,[1] and Toshio Hirano[1,2]

[1]Laboratory of Developmental Immunology, Graduate School of Frontier Bioscience and Graduate School of Medicine, Osaka University, Osaka 565-0871, Japan
[2]Laboratory for Cytokine Signaling, Institute of Physical and Chemical Research Center for Allergy and Immunology, Yokohama 230-0045, Japan

Mice homozygous for the F759 mutation in the gp130 interleukin (IL)-6 receptor subunit have enhanced gp130-mediated signal transducer and activator of transcription (STAT)3 activation and spontaneously developed a lymphocyte-mediated rheumatoid arthritis-like joint disease. Here, we show that the development of the disease is dependent on both major histocompatibility complex (MHC) II–restricted CD4$^+$ T cells and IL-6 family cytokines. In spite of the necessity for CD4$^+$ T cells, the gp130 mutation was only required in nonhemtopoietic cells for the disease. The gp130 mutation resulted in enhanced production of IL-7. Conditional knockout of STAT3 in nonlymphoid cells showed that the enhancement of IL-7 production was dependent on STAT3 activation by IL-6 family cytokines. Homeostatic proliferation of CD4$^+$ T cells was enhanced in gp130 mutant mice and acceleration of homeostatic proliferation enhanced the disease, whereas the inhibition of homeostatic proliferation suppressed the disease. Anti–IL-7 antibody treatment inhibited not only the enhanced homeostatic proliferation, but also the disease in gp130 mutant mice. Thus, our results show that autoimmune disease in gp130 mutant mice is caused by increased homeostatic proliferation of CD4$^+$ T cells, which is due to elevated production of IL-7 by nonhematopoietic cells as a result of IL-6 family cytokine–gp130–STAT3 signaling.

CORRESPONDENCE
Toshio Hirano:
hirano@molonc.med.osaka-u.ac.jp

Abbreviations used: HP, homeostatic proliferation; MEF, mouse embryonic fibroblast; RA, rheumatoid arthritis; sLN, surface LN; SPF, specific pathogen-free.

Autoimmune diseases comprise a heterogeneous group of poorly understood disorders that are controlled by genetic and environmental factors (1, 2). These diseases are most simply defined by the presence of autoimmune phenomena such as autoantibodies and/or autoreactive lymphocytes. Autoimmune diseases are generally classified into two major types: tissue specific and systemic (2, 3). In tissue-specific diseases, tissue-specific autoantibodies or tissue-specific T lymphocytes play critical roles. However, there are some atypical autoimmune diseases that cannot be classified into either of these types. For example, an arthritis observed in TNF-α AU-rich element–deleted mice can be induced by a chronic inflammatory proliferative reaction that is dependent on TNF-α but not on adaptive autoimmunity; the TNF-α–induced arthritis does not require mature lymphocytes, although these mice are positive for autoantibodies (4). Therefore, it is also possible that some cytokines, alone and in the absence of autoreactive lymphocytes, can induce tissue-specific autoimmune-like diseases (5, 6). In this regard, it is interesting that the epidermal-specific deletion of junB and c-jun molecules, which enhances the expression of many cytokines, induces psoriasis even in the absence of mature lymphocytes (7).

The immune system is well controlled to protect the host from exogenous pathogens. Because CD4$^+$ T cells are critical for controlling the adaptive immune system, maintaining a certain level of antigen-specific CD4$^+$ T cells in a peripheral pool is important for the efficient elimination of exogenous pathogens (8). CD4$^+$

The online version of this article contains supplemental material.

T cells in peripheral organs are divided into two populations according to their expression of CD44 molecules: the $CD44^{high}$ memory and $CD44^{low}$ naive phenotypes (9). It is hypothesized that the $CD44^{low}$ population consists of relative newcomers from thymus selection, whereas the $CD44^{high}$ memory cells are survivors in the peripheral environment. Especially when the peripheral T cell number is low (i.e., in the neonatal condition, or after irradiation, chemotherapy, or viral infection), both $CD4^+$ and $CD8^+$ T cells proliferate dramatically (10). This proliferation, termed "homeostatic proliferation" (HP), plays a critical role in maintaining the T cell number in the periphery (10). Homeostatic proliferating T cells show higher CD44 expression and cytokine secretion and divide faster than $CD44^{low}$ naive cells (9). Because the $CD44^{high}$ memory phenotype T cells increase with age and divide slowly, even under normal, specific pathogen-free (SPF) conditions, it is clear that HP is induced in normal healthy animals (9, 10). HP is strong in the neonatal period when thymus-derived naive T cells first migrate into the lymphopenic peripheral environment (11). Two known signals stimulate T cell HP. One is mediated by MHC–self-peptide complexes and the other is mediated by common γ cytokines, such as IL-7 and IL-15 (10, 12). In fact, $CD4^+$ T cell HP is significantly impaired in MHCII- or IL-7–deficient mice (12, 13). Furthermore, the overexpression of IL-7 in vivo induces autoimmune diseases, including dermatitis or colitis, in mice (14, 15). Recently, HP that produced IL-21 was shown to enhance autoimmune disease in NOD mice (16).

IL-6 is a pleiotropic cytokine that regulates multiple biological functions such as development of the nervous and hematopoietic systems, acute-phase responses, inflammation, and immune responses (17). In rheumatoid arthritis (RA) patients, a high concentration of IL-6 is detected in the serum and joint fluids (18). Recently, important roles for proinflammatory cytokines, such as TNF-α, IL-1, and IL-6 in the pathogenesis of RA have been reported (19, 20). The importance of IL-6 has also been shown in SKG mice, a model of spontaneously occurring RA, and in antigen-induced RA models, such as CIA and AIA (21–23). Furthermore, treatment with anti–IL-6 receptor is effective for certain patients with RA (24).There are nine IL-6 family cytokines, including IL-6, oncostatin M, LIF, CNTF, CT-1, IL-11, and IL-27 (25). All the family members share gp130 as a receptor subunit and signal transducer (17). We previously showed that gp130 transduces two major signaling pathways after stimulation with an IL-6 family cytokine. One is the JAK–STAT3 pathway, from its YxxQ motifs, and the other is the SHP2–Gab-Ras-Erk–MAPK pathway, from the Y759 residue in its cytoplasmic portion (26). To investigate the in vivo function of these signaling pathways, we have established a series of knockin mice (27) and shown that one of these lines, $gp130^{F759/F759}$ (F759), spontaneously develops an RA-like disease in a manner dependent on mature lymphocytes ∼1 yr after birth (28). The severity of the disease in the F759 is enhanced in an IL-6–dependent manner by crossing the mice with p40-Tax Tg, human T cell leukemia virus 1 transgenic mice (29).

Here, we seek to clarify the immunological mechanisms by which the $gp130^{F759/F759}$ mutation causes the RA-like disease. Our results from F759 showed the involvement of enhanced $CD4^+$ T cell HP caused by IL-6 family-gp130–STAT3–IL-7 cascade in nonhematopoietic cells bearing the $gp130^{F759/F759}$ mutation.

RESULTS

IL-6, MHCII-restricted $CD4^+$ T cells and the $gp130^{F759/F759}$ mutation in nonhematopoietic cells are involved in the development of RA-like disease

We first examined whether development of RA-like disease in F759 was dependent on IL-6. We prepared a double mutant, IL6KO/F759, and monitored its development of the disease. Both the severity and the incidence of the disease were significantly decreased in the IL-6–deficient F759 compared with control F759 (Fig. 1 A), indicating the involvement of IL-6 in disease development. However, the disease still developed in the absence of IL-6. Because the disease was dependent on the $gp130^{F759/F759}$ mutation (28), these results suggested other IL-6 family cytokines are also involved in the disease in F759.

To identify the lymphocyte populations necessary for the disease, we generated the following four double mutant mice: Igh6KO/F759, CD4KO/F759, CD8KO/F759, and C2TAKO/F759. The Igh6KO/F759 showed almost the same progression of the disease as the control F759 (Fig. 1 B), but the CD4KO/F759 had significantly less severe arthritis (Fig. 1 B). However, CD8KO/F759 had significantly increased score and incidence compared with the control mice (Fig. 1 B), showing that $CD8^+$ T cells are dispensable, or rather suppressive for disease development. We hardly detected the disease in C2TAKO/F759 (Fig. 1 B). Therefore, we concluded that MHCII-restricted $CD4^+$ T cells were necessary but that $CD8^+$ T or B cells were dispensable for the development of the arthritis in F759.

To investigate which tissues or cells needed to have the gp130 mutation for disease development, we divided all the cells in the body into two groups: hematopoietic and nonhematopoietic. We performed BM transplantation using F759 and wild-type congenic mice. Bone marrow cells derived from wild-type or F759 were transplanted into lethally irradiated wild-type or F759. Chimerism, tested using BM cells, was >95% 8 mo after transplantation (unpublished data). We observed the disease developed in the two groups of chimeric mice in which nonhematopoietic cells had the $gp130^{F759/F759}$ mutation, regardless of the presence of the $gp130^{F759/F759}$ mutation in the hematopoietic cells 8 mo after BM transplantation; that is, the disease developed in the chimeric mice in which the host was F759 and the BM donor was either wild-type or F759 (F759 having wild-type BM [62.5%, $n = 8$] and F759 having F759 BM [57.1%, $n = 7$]). Conversely, chimeric mice with a wild-type nonhematopoietic environment failed to develop the disease, regardless of the presence of the $gp130^{F759/F759}$ mutation in the hematopoietic cells (wild-type host having wild-type BM [0%, $n = 12$] and wild-type host

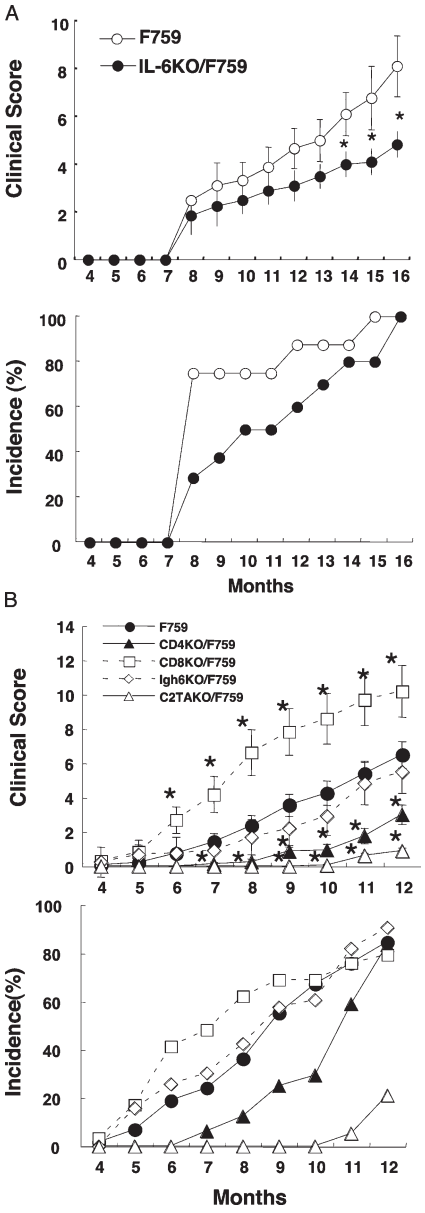

Figure 1. The arthritis of F759 is dependent on IL-6 and MHCII-restricted CD4+ T cells. (A) Clinical score and incidence of arthritis in IL-6KO/F759 (closed circles, $n = 10$) and IL-6KO hetero/F759 or F759 (open circles, $n = 10$). (top) Data are the mean ± SEM of the arthritis scores. (bottom) Incidence of arthritis with a score >4.0. The p-value was calculated by Student's *t* test. Clinical scores of 14–16-mo-old IL-6KO/F759 were significantly lower than the control. (*, $P < 0.05$) (B) Clinical scores and incidences of arthritis in Igh6KO/F759 (open diamonds, $n = 25$), CD8KO/F759 (open squares, $n = 30$), CD4KO/F759 (closed triangles, $n = 21$), C2TAKO/F759 (open triangles, $n = 19$), and F759 (closed circles, $n = 80$). (top) Data are the mean ± SEM of the arthritis scores. (bottom) Incidence of arthritis with a score >2.0. Clinical scores of 6-12-mo-old CD8KO/F759 were significantly higher (*, $P < 0.05$). Scores of 5–12-mo-old CD4KO/F759 and C2TAKO/F759 were significantly lower. (*, $P < 0.05$).

having F759 BM [0%, $n = 10$]). These results showed that the gp130$^{F759/F759}$ mutation in nonhematopoietic cells was necessary for the development of the disease. Together, these results demonstrated that MHCII-restricted CD4+ T cells were critically involved, but that the gp130 mutation in the CD4+ T cells was not necessary for the disease. Therefore, we focused next on the roles played by CD4+ T cells and nonhematopoietic cell populations bearing the gp130$^{F759/F759}$ mutation in the development of the disease in F759.

Homeostatic proliferating CD4+ T cells are involved in the disease in F759

Because King et al. recently demonstrated that HP is involved in autoimmunity in NOD mice (16) and because we observed that F759 had more memory/activated phenotype CD4+ T cells than wild-type controls (Fig. 2 A) and that F759 had significant lymphoadenopathy and splenomegaly (28), we hypothesized that enhanced HP of CD4+ T cells might be involved in the development of the disease in F759.

As expected, we found that the CD4+ T cell HP was enhanced in F759 compared with wild-type mice after irradiation (Fig. 2 B). We next modified the speed of the HP. First, we used neonatal thymectomy to enhance HP; neonatal thymectomy suppresses T cells in the thymus from entering the peripheral environment, resulting in enhanced HP in the periphery (11). Here, we chose a day-7 thymectomy (NTx) to induce HP in vivo because Asano et al. demonstrated that NTx did not reduce CD25+CD4+ T (T reg) cells numbers and did not induce any autoimmune disease, whereas a day-3 thymectomy (N3Tx) reduced the numbers of T reg cells and induced several autoimmune diseases (30). We confirmed that the CD4+ T cells in NTxed F759 divided more rapidly than those in NTxed wild-type controls or non-NTxed F759 (Fig. 2 C).

We also noted that the NTxed F759 had prominent lymphadenopathy and splenomegaly, suggesting an enhanced HP in F759 is a critical factor for determining the size of lymph nodes and spleen. The total cell number in the lymph nodes and spleen increased dramatically in F759 compared with wild-type mice after both were NTxed (Fig. 2, D and E). The numbers of CD4+ T cells in the lymph nodes and spleen increased significantly in the F759 compared with wild-type mice after NTx (Fig. 2 F). HP is reported to induce memory/activated phenotype CD4+ T cells (31). Consistent with this, the majority of the CD4+ T cells in NTxed wild-type and F759 showed the memory/activated phenotype (Fig. 2 G), suggesting that the enhanced CD4+ T HP in F759 accelerated the accumulation of memory/activated T cells.

Importantly, the NTxed F759 developed arthritis earlier than the sham-operated F759 (Fig. 3 A). We observed mononuclear cell infiltration and hyperplasia of the synovial cells in F759 after NTx (unpublished data). In contrast, we observed few signs of disease in the wild-type mice, even after NTx (Fig. 3 A). We further confirmed that the disease in the NTxed F759, like that of the untreated F759, was dependent on MHCII-restricted CD4+ T cells (Fig. 3 B).

We next investigated whether the suppression of HP in F759 inhibits development of the disease. Because we showed a large number of CD4+CD25− T cells, filler cells, suppressed

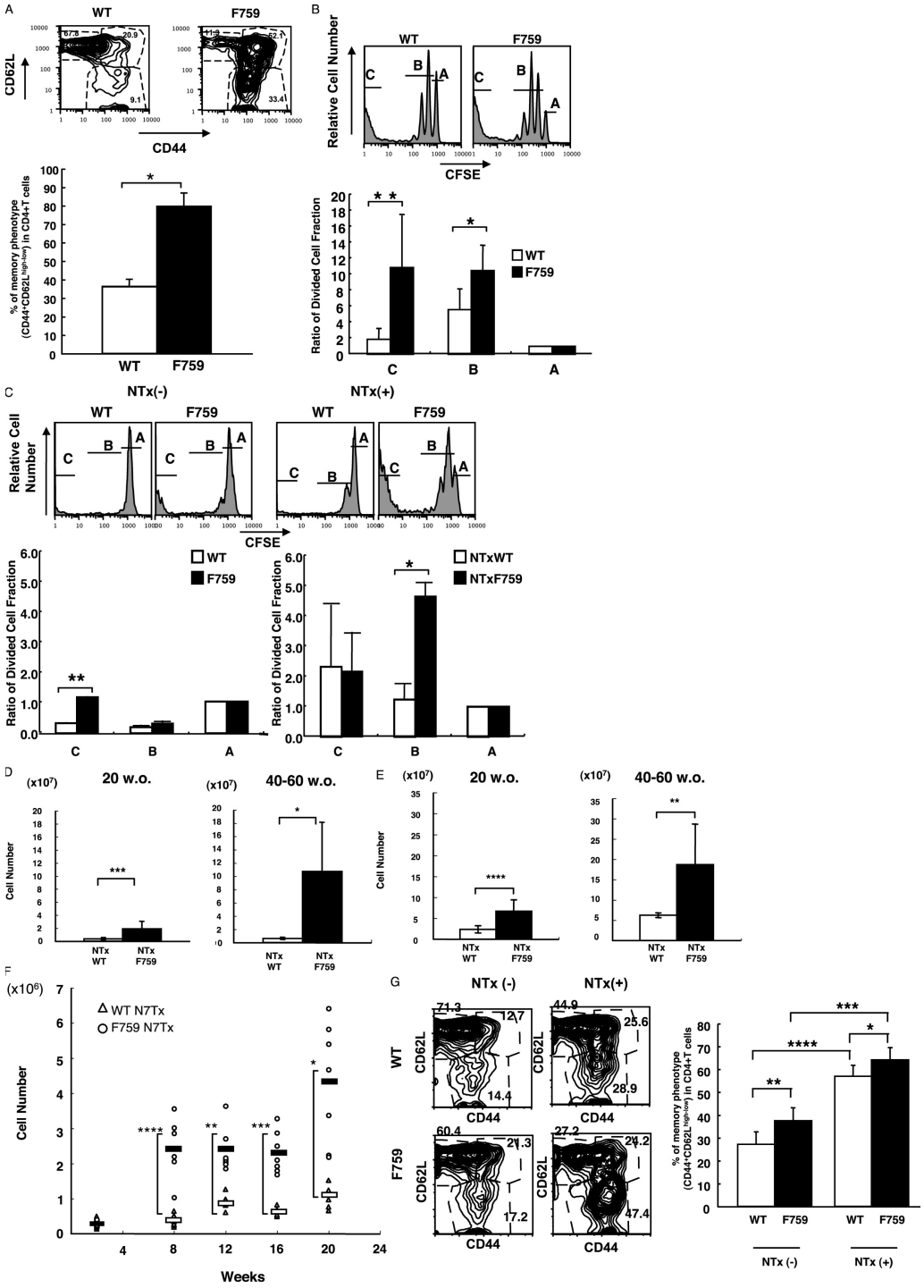

Figure 2. Increase in CD44^{high}CD4^{+} T cells, lymphadenopathy, splenomegaly, and enhanced homeostatic proliferation in the periphery of F759. (A) FACS profiles of CD4^{+} T cells isolated from sLNs of F759 and control mice (8–10 mo old). These experiments were performed three times independently; representative data are shown. The percentage of CD44^{high}CD4^{+} T cells (CD62L^{high} and CD62L^{low}) is shown with error bars indicating 1 SD. The p-value was calculated by Student's *t* test (*, P = 0.0000025). (B) CD44^{low}CD4^{+} T cells were sorted from C57BL/6/SJL mice, labeled with CFSE, and injected into irradiated wild type or C57BL/6/F759. FACS profiles of the CD45.1^{+}CD4^{+}T cells in the sLNs and spleen are shown. These experiments were performed five times independently and representative data are shown. The relative amount of CFSE^{high} (most slowly dividing [A]), CFSE^{middle} [B], and CFSE^{low} (most rapidly dividing [C]) cells, with the value for CFSE^{high} defined as 1, is shown with error bars indicating 1 SD. The p-value was calculated by Student's *t* test (*, P = 0.00037 and **, P = 0.000002). (C) CD44^{low}CD4^{+} T cells from C57BL/6/SJL were CFSE labeled and injected into nonthymectomized and N7Txed C57BL/6 or C57BL/6/F759 neonates. FACS profiles of CD45.1^{+}CD4^{+} T cells from the sLNs and spleen are shown. These experiments were performed three times independently and representative data are shown. The relative

HP (32), we transferred 3×10^7 or 3×10^6 filler T cells to inhibit the HP of $CD4^+$ T cells in the NTxed F759 neonates. As shown in Fig. 3 C, 3×10^7 filler T cells almost completely suppressed the $CD4^+$ T cell HP in NTxed F759. Moreover, we showed the injection of filler T cells significantly suppressed the disease (Fig. 3 D). Collectively, these results indicated homeostatic proliferating $CD4^+$ T cells were involved in the RA-like disease in F759.

It is well established that T reg cells play a role in various autoimmune disease developments (33). Moreover, a recent report suggested the important role of IL-6 secreted from DCs in the modulation of the T reg cell function (34). These reports suggested that a reduced T reg cell activity might cause the disease development in F759. However, this was not the case. We showed the following: (a) the percentages and numbers of $CD25^+GITR^+CD4^+$ T cells were not altered in F759 compared to control mice with or without N7Tx (Fig. S1, A and B, available at http://www.jem.org/cgi/content/full/jem.20052187/DC1, and not depicted); (b) FoxP3 expressions in $CD25^+CD4^+$ T cells did not decrease in F759 with or without N7Tx compared with these from control mice (Fig. S1 C); and (c) suppressive activity for proliferation of $CD25^-CD4^+$ T cells in vitro is not altered between T reg cells isolated from F759 with or without N7Tx and T reg cells from control mice (Fig. S1 D). With the data that (a) filler $CD4^+CD25^-$ T cells (Fig. 3 D), (b) the report by Asano et al. that T reg cell activity disappeared by N3Tx but not N7Tx (30), (c) we did not see any differences for the disease development between F759 N3Txed and N7Txed (Fig. S1 E), and (d) injection of anti–IL-2 Abs during neonatal period (which efficiently eliminates T reg cells in vivo [references 32, 35]) did not accelerate the disease in F759 (not depicted), we concluded that T reg cells have a minimum role in RA-like disease in F759 model.

The IL-6/IL-6 family-gp130–STAT3–IL-7 cascade exists in nonhematopoietic cells

We next asked whether the $gp130^{F759/F759}$ mutation in the nonhematopoietic cell population plays a role in the enhanced HP of $CD4^+$ T cells in the F759. To investigate this possibility, we first focused on IL-7 and TSLP because these cytokines are reported to enhance $CD4^+$ T cell HP (12, 36). We showed that the amount of mRNA per cell for IL-7, but not for TSLP, significantly increased in the lymphoid organs of the F759 compared with the controls (Fig. 4 A and not depicted) as well as after sublethal irradiation and NTx (Fig. 4, B and C), suggesting the $gp130^{F759/F759}$ mutation in nonhematopoietic cells affected the IL-7 expression in vivo. The IL-7 expression was correlated with IL-6 expression in the F759 (Fig. 4, C–E), suggesting the existence of a cascade for IL-6–mediated IL-7 expression.

Because the major IL-7–producing populations are reported to be nonhematopoietic cells (37), we investigated whether the IL-7–producing cells in NTxed F759 are also nonhematopoietic cells. As expected, the major IL-7–expressing cell populations in the F759 were nonhematopoietic cells (Fig. 4 F). These results suggested that IL-6 or IL-6 family cytokines acting on nonhematopoietic cells with the $gp130^{F759/F759}$ mutation resulted in the enhanced expression of IL-7 in nonhematopoietic cells. Consistent with this, IL-7 mRNA expression in the surface LNs (sLNs) (with and without irradiation) was enhanced by IL-6 in vivo (Fig. 5, A and B). Moreover, to know whether IL-6 directly induces IL-7 production in nonhematopoietic cells, we stimulated primary fibroblasts isolated from F759 and control mice with IL-6. As shown in Fig. 5 C, IL-6 significantly enhanced the expression of IL-7 mRNA in F759 fibroblasts compared with the vehicle controls. IL-6 stimulation showed little effect on IL-7 expression in control fibroblasts (Fig. 5 C), but it significantly induced IL-7 in the presence of soluble receptor of IL-6 (Fig. 5 D).

It is known that IL-6 family cytokines such as IL-11, CT-1, OSM, and LIF share gp130 as a signal transducer (25). Moreover, because we showed that IL-6 just partially plays a role in the disease development in F759 (Fig. 1 A), other IL-6 family cytokines were suggested to be involved in disease development. Therefore, we hypothesized that not only IL-6 but also other IL-6 family members induced IL-7, which is a critical factor for disease development. In fact, sIL-6R plus IL-6, OSM, LIF, IL-11, or CT-1 induced IL-7 mRNA in primary fibroblasts (Fig. 5 E and not depicted). We hypothesized that gp130-STAT3 signaling, but not gp130-SHP2/MAPK, plays an important role for IL-7 expression because F759 fibroblasts, which are defective of the gp130-SHP2/MAPK pathway but show an enhanced gp130–STAT3 pathway as the result of Y759F mutation, expressed more IL-7 after IL-6 treatment compared with control (Fig. 5 C). Consistent with this, IL-6 plus sIL-6R stimulation failed to induce IL-7 mRNA in mouse embryonic fibroblasts (MEFs) prepared

amount of $CFSE^{high}$ (A), $CFSE^{middle}$ (B), and $CFSE^{low}$ (C) cells, with the value for $CFSE^{high}$ defined as 1, is shown with error bars indicating 1 SD. The p-value was calculated by Student's *t* test (*, $P = 0.0017$ and **, $P = 0.0008$). (D and E) The sLNs (D) and spleen (E) were from and the total cell numbers were calculated. The mean is shown with error bars indicating 1 SD. The p-value was calculated by Student's *t* test (*, $P = 0.0042$; **, $P = 0.0038$; ***, $P = 0.00034$; and ****, $P = 0.00027$). (F) The sLNs and spleen were harvested from NT7xed C57BL/6 and C56BL/6/F759. The numbers of $CD4^+$ T cells were calculated from FACS analyses (open circles; N7Txed F759 and open triangles; N7Txed wild type). The mean is shown as open (N7Txed wild type) and closed (N7Txed F759) bars. The p-value was calculated by Student's *t* test (*, $P = 0.0065$; **, $P = 0.0068$; ***, $P = 0.00034$; and ****, $P = 0.00021$). (G) Neonatal thymectomy increased the $CD44^{high}$ memory/activated $CD4^+$ T cells in the spleen of NTx F759. FACS profiles of $CD4^+$ T cells isolated from the spleen of N7Txed or sham-N7Txed F759 and wild-type mice (2 wk old). These experiments were performed twice independently (total 12 samples each) and representative data are shown. The percentage of $CD44^{high}CD4^+$ T cells ($CD62L^{high}$ and $CD62L^{low}$) is shown with error bars indicating 1 SD. The p-value was calculated by Student's *t* test (*, $P = 0.024$; **, $P = 0.0032$; ***, $P = 0.00000039$; and ****, $P = 0.0000002$).

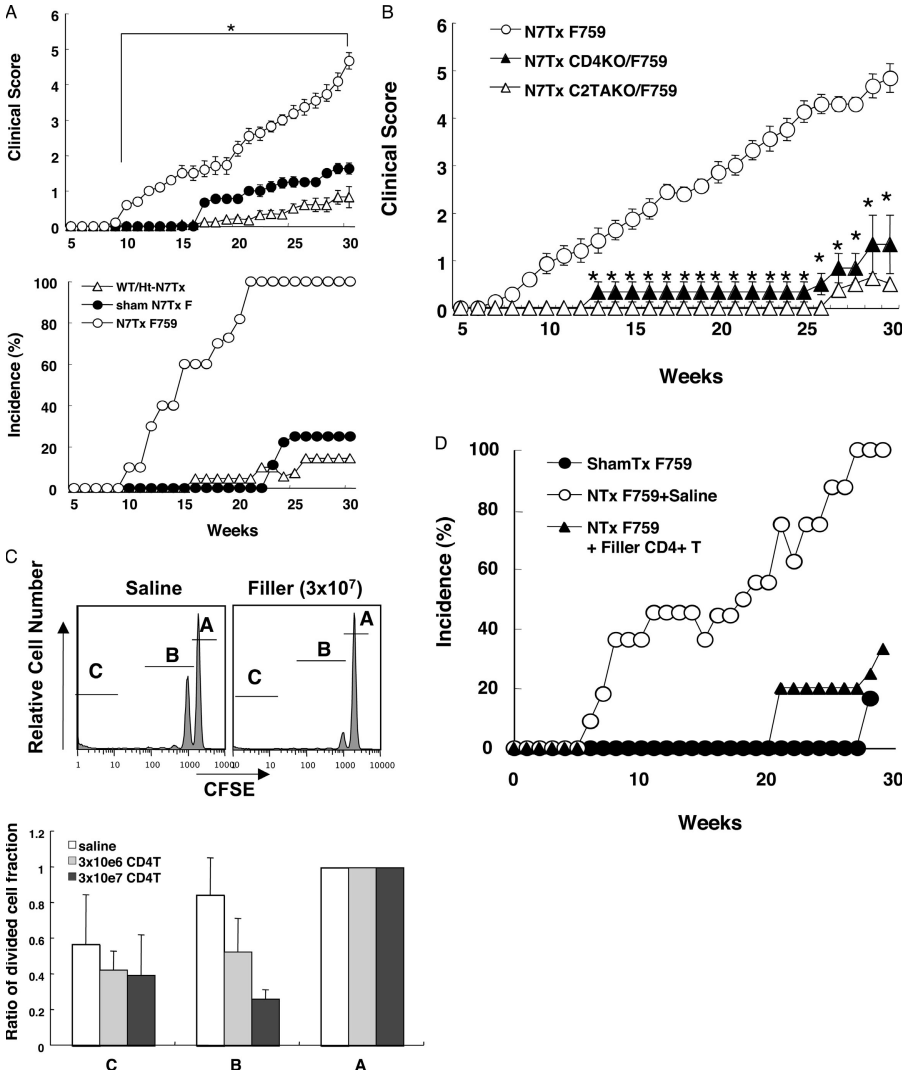

Figure 3. CD4$^+$ T cell homeostatic proliferation played a critical role for the disease development in F759. (A) Clinical score and incidence of arthritis in N7Txed F759 (open circles, $n = 30$), F759 hetero or N7Txed wild-type (open triangles, $n = 24$), and sham-Txed F759 (closed circles, $n = 20$). (top) Data are the means ± SEM of the arthritis scores. (bottom) Incidence of arthritis with a score >2.0. Clinical scores of 10–30-wk-old N7TxF759 were significantly higher than the sham N7Tx ones (*, $P < 0.05$). (B) Data are the means ± SEM of the arthritis score in N7Txed F759 (open circles, $n = 12$), N7Txed CD4KO/F759 (closed triangles, $n = 12$), and N7Txed C2TAKO/F759 (open triangles, $n = 12$). Clinical scores of N7Txed CD4KO/F759 and N7Txed C2TAKO/F759 (13–30 wk old) were significantly milder than N7Txed F759 ones (*, $P < 0.05$). (C) CD44^{low}CD4$^+$ T cells from C57BL/6/SJL were labeled with CFSE and injected i.v. with or without filler T cells injected i.p. into N7Txed C57BL/6/F759 neonates. FACS profiles of CD45.1$^+$CD4$^+$ T cells from sLNs and spleen are shown. These experiments were performed three times independently and representative data are shown. The relative amount of CFSE^{high} (A), CFSE^{middle} (B), and CFSE^{low} (C) cells, with the value for CFSE^{high} defined as 1, is shown with error bars indicating 1 SD. (D) Incidence of arthritis with a score >2.0 in N7Txed F759 plus saline (open circles, $n = 14$), N7Txed F759 plus i.p. injection of filler T cells (closed triangles, $n = 14$) and sham-N7Txed F759 (closed circles, $n = 15$).

from gp130$^{FxxQ/FxxQ}$ knockin (FxxQ) mice, which are defective in gp130-meditaed STAT3 activation (27) (Fig. 5 F, top left, and not depicted). Additionally, we showed that IL-7 protein increased in MEF from F759 compared with wild-type controls after stimulation of IL-6 plus sIL-6R (Fig. 5 G). We performed a critical experiment using type I–collagen–Cre/STAT3$^{flox/flox}$ mice (Col1a-STAT3). IL-6 plus sIL-6R stimulation did not induce IL-7 expression in vitro in lymph nodes of Col1a-STAT3 (Fig. 5 F, top right). Moreover, in vivo expression of IL-7 in lymph nodes of irradiated Col1a-STAT3 was significantly lower compared with controls (Fig. 5 F, bottom). Furthermore, we showed there is almost no IL-7 protein expression in lymph nodes of Col1a-STAT3 after irradiation (Fig. 5 H). Together with the existence of a STAT3 binding site in the IL-7 promoter region (unpublished data), these results indicated that the IL-6/IL-6 family-gp130-STAT3-IL-7 cascade existed in the nonhematopoietic cells.

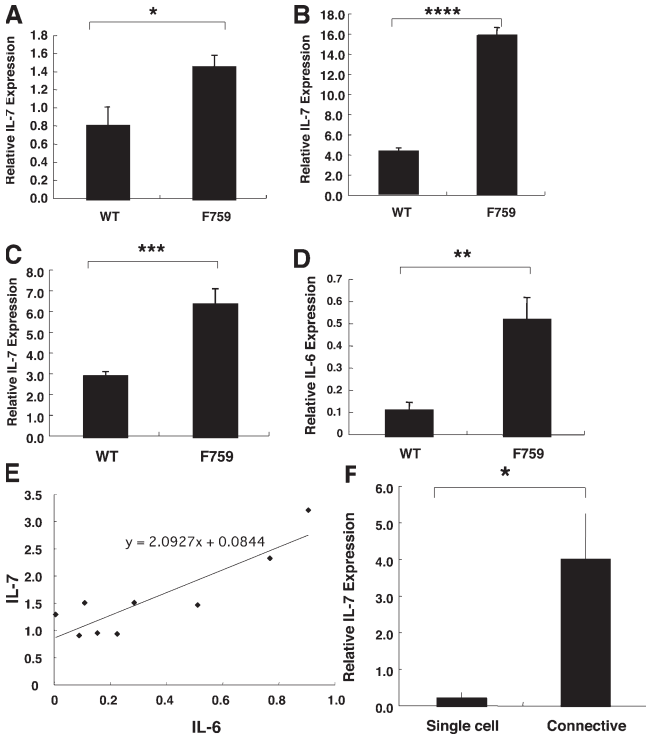

Figure 4. Increased IL-7 expression in nonhematopoietic cells in F759. (A) The sLNs were harvested from wild-type C57BL/6 and C57BL/6/F759. Real-time PCR for IL-7 was performed. (B) The sLNs were harvested from wild-type C57BL/6 and C57BL/6/F759 10 d after irradiation. Real-time PCR was performed for IL-7. (C and D) The sLNs were harvested from N7Txed wild-type C57BL/6 and C57BL/6/F759 10 d after N7Tx. Real-time PCR was performed for IL-7 (C) and IL-6 (D). The mean is shown with error bars indicating 1 SD. The p-value was calculated by Student's *t* test (*, P = 0.0021; **, P = 0.011; ***, P = 0.00041; and ****, P = 0.000000003). These experiments were performed three times independently and representative data are shown. (E) The correlation between relative IL-7 and IL-6 expression in N7Txed wild-type or F759 is shown. The correlation efficiency was 0.88. (F) The sLNs were harvested from C57BL/6/F759. The cell strainer pass-through and the retained fractions were prepared. Real-time PCR was performed for IL-7. The mean is shown with error bars indicating 1 SD. The p-value was calculated by Student's *t* test (*, P = 0.0021). These experiments were performed three times independently and representative data are shown.

IL-7 expression is involved in enhanced CD4$^+$ T cell HP and is necessary for the development of the disease in F759 neonates

We next asked whether the enhanced CD4$^+$ T cell HP in F759 is dependent on an enhanced production of IL-7. We transferred CFSE-labeled CD4$^+$ T cells into F759 neonates 1 d after NTx and injected an anti–IL-7 antibody. The in vivo depletion of IL-7 by the antibody treatment strongly suppressed CD4$^+$ T cell HP in the F759 neonates, whereas the IL-7 depletion in wild-type controls showed a minimal effect on CD4$^+$ T cell HP, as demonstrated by Min et al. (reference 11 and Fig. 6 A), showed an enhanced IL-7 production via gp130 signaling was involved in the enhanced HP of CD4$^+$ T cells in F759 neonates.

Finally, we analyzed the contribution of IL-7 on the development of the disease in NTxed F759. We showed that the anti–IL-7 antibody that significantly inhibited the gp130$^{F759/F759}$-mediated enhancement of CD4$^+$ T cell HP almost completely suppressed the disease in NTxed F759, whereas control IgG2b had no effect on the disease development (Fig. 6 B and not depicted). We could not suppress the disease development after injection of anti–IL-7 antibody in the neonatal period of F759 without a thymectomy (unpublished data). This ineffectiveness of the antibody treatment might be a result of the difficulty to maintain enough amount of anti–IL-7 antibody in vivo during a long period, such as 1 yr. However, we showed that IL-7RKO/F759 did not develop the disease in age (the disease incidence was 11% in IL-7RKO/F759 and 84% in control F759 mice at 12 mo old [$n = 8$ and $n = 12$, respectively]). From all the aforementioned results, we concluded that, in the F759, the overexpression of IL-7 mediated through the IL-6/IL-6 family-gp130–STAT3 signaling in nonhematopoietic cell populations was involved in both the accelerated HP of CD4$^+$ T cells and disease development.

DISCUSSION

We demonstrated previously that Rag2KO background F759 did not develop the disease (28), clearly indicating that mature lymphocytes, CD4$^+$ T cells, CD8$^+$ T cells, and B cells are responsible for disease development. Here, we neglected the possible involvement of CD8$^+$ T cells and B cells for the enhancement of the disease. CD8$^+$ T cells are suppressive, although the mechanism of this phenomenon of CD8$^+$ T cells should be clarified by additional studies after confirming it. From these results, it is reasonable to conclude that CD4$^+$ T cells play a role in the disease of F759. In fact, we showed significant reduction of the disease severity in CD4-deficient F759 compared with control F759, indicating that, at least in part, CD4$^+$ T cells are involved in the disease. We should note that CD4-deficient mice contain T cells able to recognize MHCII molecules (38). This may explain why the disease developed without CD4$^+$ cells.

We observed that CIITAKOF759 clearly prevented induction of the disease, whereas CD4-deficient F759 animals show less protection from the disease. We hypothesize three possibilities to explain this phenomenon. First, as we described in previous paragraphs, CD4-deficient mice contain many T cells able to recognize MHCII molecules (38), whereas there is a limited number of MHCII-restricted CD4$^+$ T cells in CIITAKO mice. Second, it is known that CIITA can influence transcription of MHCII plus multiple accessory genes for MHCII antigen presentation including H2DM, Ii, Plexin A1, and cathepsin E (39–41). Because accessory molecules are not able to work for CD4$^+$ T cell responses without MHCII molecules, a reasonable primary defect of CIITA is MHCII deficiency in antigen-presenting cells. However, it was also reported that CIITA induces MMP9 and collagen (COL1A2) transcriptions (42, 43). In the case of these two genes, their expression levels in synovial cells derived from F759 were not changed compared with wild-type controls

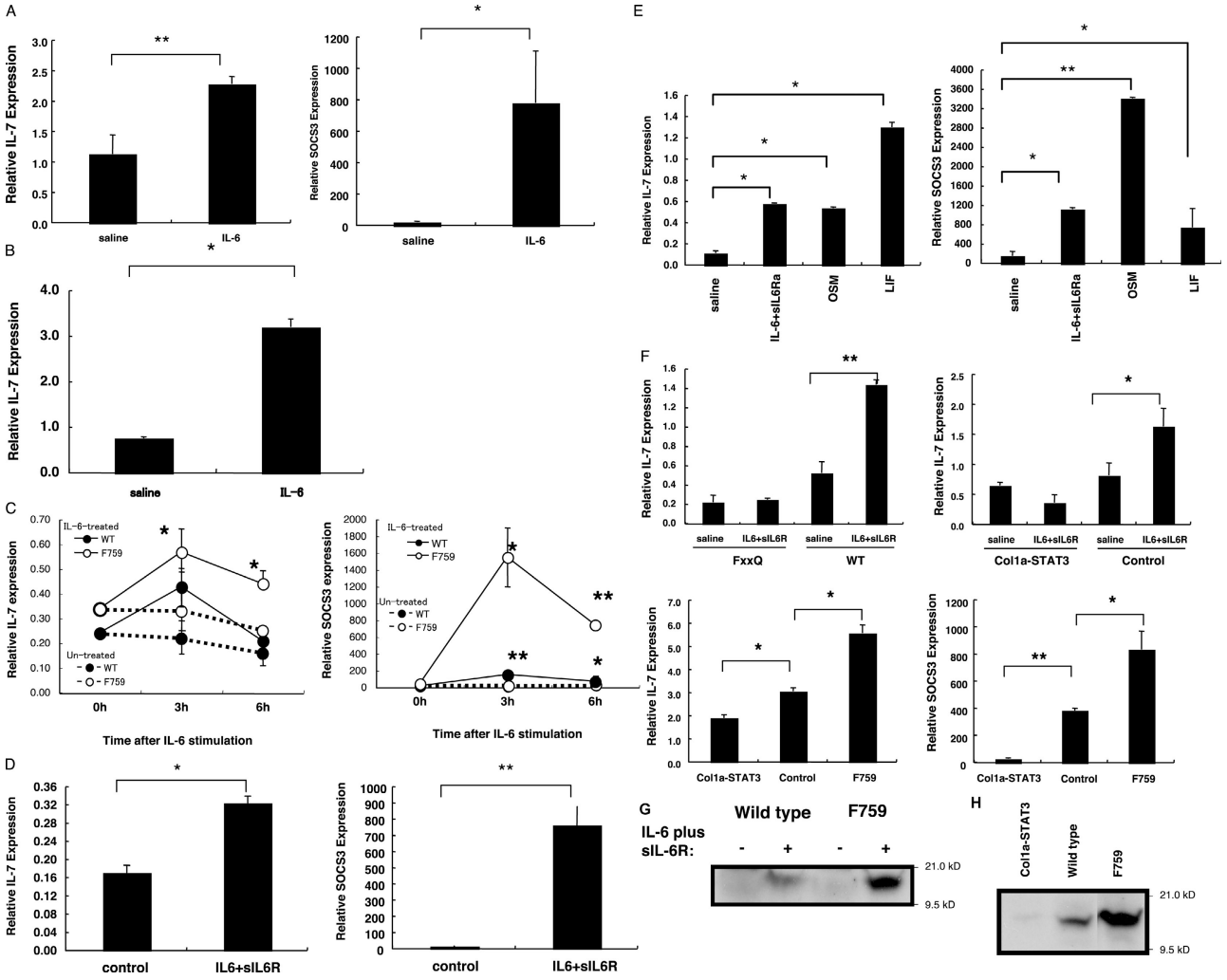

Figure 5. IL-6 injection induced IL-7 in vivo and gp130–STAT3 directly induced IL-7 in the fibroblasts of F759. (A) IL-6KO/F759 (nonirradiated) with i.v. injection IL-6 was prepared. Real-time PCR for IL-7 or SOCS3 was performed using RNA from the sLNs of the IL-6KO/F759. These experiments were performed two times independently and the sum of the data is shown. (B) IL-6 KO mice with irradiation 24 h before the i.v. injection of IL-6 was prepared. Real-time PCR for IL-7 was performed using RNA from the sLNs. These experiments were performed three times independently and representative data are shown. The p-value was calculated by Student's *t* test (in A: *, $P = 0.034$; **, $P = 0.018$). In B, *, $P = 0.016$. (C) Splenic fibroblasts were prepared and stimulated with IL-6. Real-time PCR was performed for IL-7 and SOCS3. The mean is shown with error bars indicating 1 SD. Student's *t* test was done between IL-6–treated and untreated cells. The p-value was calculated by Student's *t* test (*, $P < 0.05$ and **, $P < 0.01$). These experiments were performed three times independently and representative data are shown. (D) Splenic fibroblasts prepared from wild-type neonates were stimulated with IL-6 plus sIL-6R. Real-time PCR was performed for IL-7 and SOCS3. The mean is shown with error bars indicating 1 SD. The p-value was calculated by Student's *t* test (*, $P = 0.010$ and **, $P = 0.014$). These experiments were performed three times independently and representative data are shown. (E) Splenic fibroblasts from F759 were stimulated with IL-6 plus sIL-6R, OSM, and LIF. Real-time PCR was performed for IL-7 and SOCS3. The mean is shown with error bars indicating 1 SD. The p-value was calculated by Student's *t* test (*, $P < 0.05$ and **, $P < 0.01$). These experiments were performed three times independently and representative data are shown. (F, top left) MEF were prepared from FxxQ or wild-type fetus were stimulated with IL-6 plus sIL-6R. Real-time PCR was performed for IL-7. The mean is shown with error bars indicating 1 SD. The p-value was calculated by Student's *t* test (**, $P < 0.01$). These experiments were performed three times independently and representative data are shown. (top right) Col1a-STAT3, control ($STAT3^{flox/flox}$ or type I-collagen-Cre/$STAT3^{flox/+}$), and F759 were irradiated, and the sLNs were harvested and cultured with IL-6 plus sIL-6R. Real-time PCR for IL-7 was performed using sLNs. The mean is shown with error bars indicating 1 SD. The p-value was calculated by Student's *t* test (*, $P < 0.05$). These experiments were performed three times independently and representative data are shown. (bottom) Col1a-STAT3, control, and F759 were irradiated. Real-time PCR for IL-7 or SOCS3 was performed using the lymph nodes. The mean is shown with error bars indicating 1 SD. The p-value was calculated by Student's *t* test (*, $P < 0.05$; **, $P < 0.01$). These experiments were performed three times independently and representative data are shown. (G) MEF were prepared from F759 or wild-type fetus were stimulated with IL-6 plus sIL-6R. Their protein fractions were prepared and applied on SDS-page followed by Western blotting of IL-7. (H) The sLNs irradiated Col1a-STAT3, wild-type, and F759 were harvested. Their protein fractions were prepared and applied on SDS-page followed by Western blotting of IL-7.

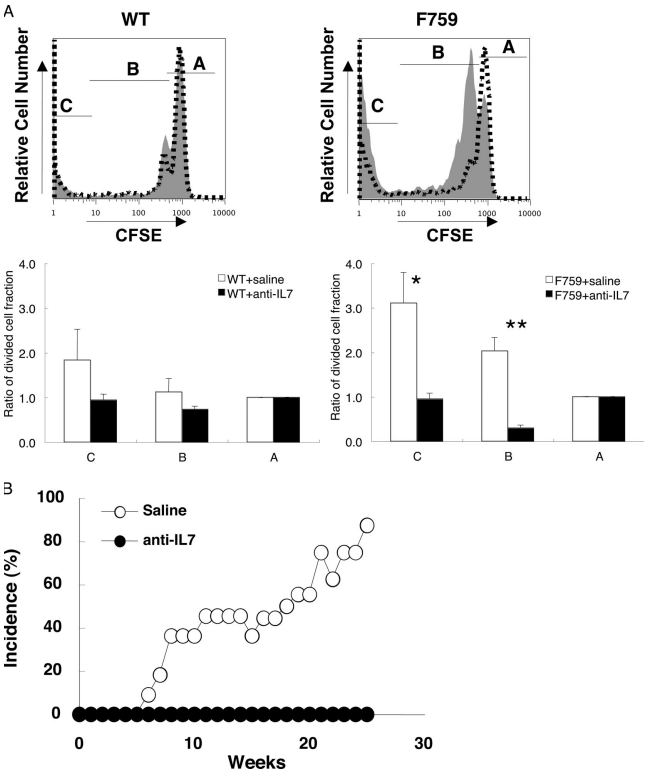

Figure 6. IL-7 expression was involved in the enhanced CD4$^+$ T cell HP and was necessary for development of the disease in F759 neonates. (A) CD44^{low}CD4$^+$ T cells were sorted from C57BL/6/SJL mice, labeled with CFSE, and injected into N7Txed C57BL/6 or C57BL/6/F759 neonates 8 d after birth. Anti–IL-7 antibody (dotted lines) or control IgG2b antibody (shaded profiles, 0.1 mg/each) was i.p. injected. The sLNs and spleen were harvested 14 d after T cell injection and FACS profiles of CD45.1$^+$CD4$^+$ T cells are shown. These experiments were performed three times independently and representative data are shown. The relative amount of CFSE^{high} (A), CFSE^{middle} (B), and CFSE^{low} (C) cells, with the value for CFSE^{high} defined as 1, is shown with error bars indicating 1 SD. The p-value was calculated by Student's *t* test (*; P = 0.012; **, P = 0.00023). (B) Incidence of arthritis with a score >2.0 in N7Txed F759 plus saline (open circles) or N7Txed F759 plus anti–IL-7 antibody (closed circles).

(unpublished data). Third, enhanced HP of T cells accelerates the disease, whereas either filling the filler CD4$^+$ T cells or anti–IL-7 treatment, which prevents the HP of CD4$^+$ T cells, suppressed the disease. These results further support the involvement of CD4$^+$ T cells in the disease, although we cannot completely neglect the possible involvement of unknown genes controlled by CIITA.

We showed that the enhanced CD4$^+$ T cell HP that is induced by gp130–STAT3-mediated IL-7 expression in nonhematopoietic cells is critical for the development of the disease in F759. Significant HP occurs at the beginning of life in neonates, but HP lasts in adults even under SPF conditions (10, 11). We showed that CD4$^+$ T cell HP was enhanced in both the neonates and adults of F759 compared with wild-type controls. Importantly, we showed that the enhanced HP in the F759 was involved in the development of the disease. There are three observations that directly support this conclusion. First, thymectomy in the neonatal period enhanced both the CD4$^+$ T cell HP and the development of the disease. Second, either the transfer of filler CD4$^+$ T cells or, third, the depletion of IL-7 inhibited the CD4$^+$ T cell HP and suppressed the disease.

How is the HP of CD4$^+$ T cells enhanced in F759? The rate of HP is known to be dependent on both TCR-MHC and cytokine signaling (12, 13, 44). We identified IL-7 from nonhematopoietic cell populations as a key cytokine for enhancing the HP of CD4$^+$ T cells in F759. Because it was an unexpected finding that gp130 signaling induced IL-7, we performed eight independent experiments to show the existence of this pathway. First, it is reported that the main source of IL-7 is nonhematopoietic cells (37), and we confirmed a connective tissue-enriched fraction, which mainly consisted of nonhematopoietic cells, expressed IL-7 in F759. Second, we showed the IL-7 mRNA and protein expression increased in F759, especially after induction of HP. Third, conversely, IL-7 mRNA and protein expression was significantly decreased in Col1a-STAT3. Fourth, we confirmed both splenic fibroblasts and MEF expressed IL-7 after stimulation of gp130 signaling. Fifth, STAT3 binding sites of gp130 were critical for IL-7 mRNA expression in MEFs after IL-6 plus sIL-6R stimulation. Sixth, IL-6 injection induced IL-7 expression in lymph nodes in vivo. Seventh, we showed IL-7 protein increased in MEFs from F759 compared with these from wild-type controls after stimulation of IL-6 plus sIL-6R. Eighth, IL-7 depletion suppressed the HP of CD4$^+$ T cells in F759. Thus, we concluded that a gp130–STAT3–IL-7 cascade in nonhematopoietic cells is critical for the enhancement of CD4$^+$ T cell HP in F759.

Because we showed that the disease development was at least in part dependent on IL-6, consistent with our previous observation that the human T cell leukemia virus 1 p40Tax-induced enhancement of the disease in F759 is dependent on IL-6 (29), we suggest that IL-6 is at least partly involved in the gp130-mediated IL-7 expression in vivo. There are nine IL-6 family members reported, which include IL-6, IL-11, IL-27, oncostatin M, LIF, and CNTF (25). Because all of their receptors share gp130 as a subunit, it is likely that other IL-6 family cytokines also play a role in the gp130–STAT3–IL-7 cascade. Therefore, we hypothesized that the reason why we had significant numbers of animals that developed the disease even in the absence of IL-6 is that other IL-6 family members function as IL-7 inducers in IL-6KO/F759. Consistent with this hypothesis, we showed that other IL-6 family members induced a significant level of IL-7 in primary fibroblasts. We also showed HP increased IL-6 expression in vivo in the F759. Interestingly, we also showed IL-7 expression was correlated with IL-6 expression in the F759 thymectomized.

How does the enhancement of CD4$^+$ T cell HP induce the disease in F759? We have not detected a bias of the T cell receptor repertoire toward CD4$^+$ T cells in F759 with the disease (unpublished data), although the memory/activated CD4$^+$ T cells were increased in F759. At present,

we cannot completely exclude the possibility that a minor population of antigen-specific $CD4^+$ T cells among the homeostatic proliferating T cells plays a pathogenic role, but our data strongly support the idea that nonspecific antigen-proliferating $CD4^+$ T cells play a central role in causing the tissue-specific RA-like disease via HP in a manner dependent on the $gp130^{F759/F759}$ mutation of nonhematopoietic cells. In this regard, it is also interesting that B cells are not required for the disease in F759, although abundant autoantibodies are produced in these mice (28). This finding suggests that the apparent adaptive autoimmunity, such as autoantibody production, observed in the F759, is merely a consequence of the inflammatory response of the disease. We hypothesize that the HP-mediated activation of $CD4^+$ T cells in F759 is a critical inducer or source of cytokines for the induction of the disease because the HP of $CD4^+$ T cells is a type of $CD4^+$ T cell activation in vivo and induces the expression of many cytokines from themselves and from DCs (45, 46).

As for the role of the IL-6 family cytokines, we propose two possibilities. One is that IL-6 family cytokines act only as a stimulator of $CD4^+$ T cell HP through IL-7 production, but not as an effector molecule for disease induction. In this case, it may be possible that some cytokines other than IL-6 family cytokines that are induced by the enhanced HP of $CD4^+$ T cells function as effectors for the disease development. The second scenario is that IL-6 family cytokines act not only as a stimulator of the HP of $CD4^+$ T cells but also as a direct effector molecule for disease induction. If the second scenario is fit to this F759 model, IL-6/IL-6 family–mediated $gp130^{F759/F759}$ signaling in nonhematopoietic tissues, most likely in the joint, could play a major role in the development of the disease. Because IL-6 is known to be a survival factor for synovial fibroblastic cells in the presence of soluble IL-6 receptor (47) and activated $CD4^+$ T cells express IL-6 family cytokines (unpublished data), it is likely that a hyperactivated STAT3 status caused by $gp130^{F759/F759}$ signaling is involved in the bone destruction or overproliferation of synovial fibroblastic cells in the F759. Such aberrant $gp130^{F759/F759}$ signaling directly or indirectly induced in joints via the enhanced HP of $CD4^+$ T cells in F759 could cause tissue-specific diseases.

Nevertheless, we emphasize that MHCII-restricted $CD4^+$ T cells were required for the disease in the F759. This may indicate that we should consider the environmental factors that cooperate with genetic factors to promote autoimmune diseases in patients. We hypothesize that certain environmental factors, including infectious agents, may induce the activation of $CD4^+$ T cells in a manner dependent on MHCII molecules. If this event causes T cell activation, resulting in the production of critical cytokines, which might be IL-6 family cytokines, at high enough levels to affect the survival and growth of the target tissue or induce chronic inflammation in the target tissue of a certain genetic background, the disease would be caused in a manner associated with MHCII as well as multiple genetic backgrounds that may affect the target tissue, as reported for many autoimmune diseases, including RA.

MATERIALS AND METHODS

Mice. F759 and FxxQ that have a human version of gp130 (S710L) were established as described previously (27). C57BL/6 were obtained from SLC. 129/B6-F759 or 129/B6-FxxQ heterozygous were crossed with C57BL/6 over more than eight generations (N8). FxxQ homozygous mice were used at 14–15 d post-coitus as a result of the perinatal lethality. C57BL/6 background Igh6KO, CD4KO, CD8KO, and C2TAKO mice were purchased from The Jackson Laboratory and C57BL/6 background IL-6KO was provided by Dr. Iwakura (University of Tokyo, Tokyo, Japan). IL-7RKO was provided by Dr. Ikuta (Kyoto University, Kyoto, Japan). These mice were crossed with C57BL/6 F759 (N8) to obtain double mutant mice: Igh6KO/F759, CD4KO/F759, CD8KO/F759, C2TAKO/F759, IL-6KO/F759, and IL-7RKO/F759. C57BL/6/SJL was also purchased from The Jackson Laboratory. $STAT3^{flox/flox}$ mice were provided by Dr. Akira (Osaka University, Osaka, Japan). Alfa I collagen-Cre mice were provided by Dr. Karsenty (Baylor College of Medicine, Houston, TX). All mice were maintained under SPF conditions according to the instructions of the Osaka University Medical School. All animal experiments were performed following the guidelines of the Institutional Animal Care and Use Committees in Graduate School of Frontier Bioscience and Graduate School of Medicine, Osaka University.

Neonatal thymectomy. Neonatal thymectomy was performed as described previously (30). In brief, C57BL/6 day 3 or day 7 neonates were anesthetized on ice and surgically thymectomized. Both lobes of the thymus were completely ablated with sterile toothpicks. The sternum and skin were sewed with 7–0 surgical sutures (Akiyama-Seisausho). Some neonates, whose skin and sternum were cut and sewn, were used as sham-operated mice.

Assessment of arthritis. Mice were inspected every week for up to 16 mo and assessed for signs of arthritis basically as described previously (28, 29). We modified the method minorly. Although we had removed scores of dead mice from the assessment, which usually had high scores (28, 29), here, we put the same scores from the point of time at which they were moribund or dead until end point of the assessment of the groups. The arthritis score shown is the sum of the scores for four limbs graded from 0 to 4. Thus, the maximum arthritis score for all four limbs was 16.

Histological analysis. Joints were fixed in 4% paraformaldehyde, decalcified for 12 h in Morse's solution (22.5% bornyl formate and 10% sodium acid citrate solution) followed by 12 h in 4% paraformaldehyde, and embedded in paraffin; sections were stained with hematoxylin/eosin (28).

BM transplantation. F759 and wild-type mice were irradiated (9.5 Gray) 24 h before bone marrow injection. BM cells (2×10^6) were prepared from congenic-SJL or -F759 and intravenously injected into the irradiated host mice. 8 mo after the injection, >95% of the bone marrow cells were replaced with the donar (CD45.1) cells (unpublished data).

Antibodies and reagents. Antibodies against FITC-conjugated anti–mouse CD19, NK1.1, $I\text{-}A^b$, PE-conjugated anti–mouse CD4, Cychrome-conjugated anti–mouse CD4, Gr-1, and CD11b, and allophycocyanin-conjugated anti–mouse CD45.1 were purchased form eBioscience. Purified anti–mouse CD3ε, CD28, FITC-conjugated anti–mouse CD44, CD45.2 and PE-conjugated anti–mouse CD25 were obtained from Caltag. PE-conjugated anti–mouse CD62L was obtained from BD Biosciences. FITC-conjugated anti–mouse GITR was obtained from R&D Systems. Anti–IL-7 antibody (mouse IgG2b) was purified from M25 hybridoma culture supernatant. The M25 hybridoma was a gift from Dr. Marrack (National Jewish Medical and Research Center, Denver, CO). Control mouse IgG2b was purchased from Sigma-Aldrich.

Cell preparation and cell sorting. The LNs (inguinal, axillaries, cervical, and mesenteric) and spleen were harvested, passed through a 100-μm cell strainer (BD Falcon) with RPMI 1640, and washed. Erythrocytes were eliminated with 0.165 M NH_4Cl. A T cell–enriched sample was prepared using a nylon wool column, and the $CD4^+CD44^{low}$ or $CD4^+CD25^-$ T cells

were purified by a Moflo high-performance cell sorter (DakoCytomation). The purity of the $CD4^+$ T cells was consistently >98%.

Flow cytometry. For cell surface staining, 10^6 T cells were incubated with fluorescence-conjugated antibodies for 30 min on ice. The cells were analyzed by flow cytometry (BD Biosciences) using CELLQuest and Flowjo software.

In vivo IL-6 and anti–IL-7 antibody treatments. 1 μg of human IL-6 (Toray) was intravenously injected into irradiated IL-6KO adult mice or nonirradiated IL-6KO/F759 (2 wk old). Anti–IL-7 antibody (0.1 mg) or mouse IgG2b antibody (0.1 mg) was intraperitoneally injected into 7-d-old neonatal thymectomized F759 every 2 d for 2 wk.

Homeostatic proliferation assay. $CD44^{low}CD4^+$ T cells (10^6) were labeled with CFSE (Invitrogen) and i.p. injected into thymectomized neonates or sublethally irradiated (5.0 Gray) adult mice. In some experiments, filler $CD25^-CD4^+$ T cells were injected i.p. to inhibit HP in vivo. The recipient neonates were killed at day 14 and recipient adults were killed on day 9 for analysis of the cell division.

In vitro T cell proliferation assay. Sorted $CD4^+CD25^-$ T cells (5×10^4) were cultured with 30 Gray irradiated splenocytes (5×10^4) in the presence of the indicated numbers of $CD4^+CD25^+$ T cells and anti-CD3e plus anti-CD28 mAbs (0.5 μg/ml each) in 96-well U-bottom plates for 72 h at 37 degree/5% CO_2. All cell populations were sorted from wild-type C57BL6 or F759 by Moflo. Cell proliferation was analyzed by TetraColor ONE (Seikagaku Corp.).

Fibroblast culture and stimulation. For splenic fibroblast, neonatal spleens (3 d after birth) of wild type and F759 were harvested and single cells were cultured in RPMI 1640 carrying 20% FCS. The medium was changed every week for 3 wk, as described previously (48). For MEFs, wild-type and FxxQ fetus (14–15 d post-coitus) were cultured in RPMI 1640 containing 10% FCS and 1 mg/ml collagenase (Roche) in 5% CO_2 incubator for 15 min. After washing the fetus twice with plain RPMI 1640, the suspensions of cells were prepared by cell strainer (BD Biosciences) and cultured in RPMI 1640 containing 10% FCS for 5 d. The resulting MEFs (5×10^5/well) were plated in six-well plates and stimulated with IL-6 plus sIL-6R (50 ng/ml each) for 6 h after 24 h of starvation in RPMI 1640 plus 0.1% FCS. Human IL-6 (Toray), human soluble IL-6 receptor (R&D Systems), mouse oncostatin M (R&D Systems), mouse CT-1 (R&D Systems), mouse IL-11 (R&D Systems), and mouse LIF (Chemicon) were used for the experiments (50 ng/ml each).

In vitro whole lymoph node culture and stimulation. The sLNs isolated from 5 Gray irradiated adult Col1a-STAT3 or controls were cut into <1-mm pieces and incubated in RPMI 1640 carrying 0.1% FCS in 5% CO_2 incubator for 3 h with or without treatment of IL-6 plus sIL-6R (50 ng/ml each).

Real-time PCR. Gene Amp 5700, SYBER green PCR Master Mix (ABI Warrington) was used for IL-6 mRNA and SOCS3 quantification. Taqman Universal PCR Master Mix (Applied Biosystems) was used for IL-7 mRNA and Foxp3 mRNA quantification. The mRNAs were prepared from purified $CD4^+$ T cells or a mixture of sLNs using Sepasol-RNA I (Nakalai), RNA-mini preparation kit (QIAGEN), RNase free DNase kit (QIAGEN), and used for the synthesis of cDNAs. The combinations of PCR primers and Taqman probes for real-time PCR were as follows: HPRT primers; 5′-GATTAGCGATGATGAACCAGGTT-3′ and 5′-CCTCCCATCTCCTTCATGACA-3′; IL-6 primers, 5′-GAGGATACCACTCCCAACAGACC-3′ and 5′-AAGTGCATCATCGTTGTTCATACA-3′; SOCS3 primers, 5′-GCGAGAAGATTCCGCTGGTA-3′ and 5′-CGTTGACAGTCTTCCGACAAAG-3′; β-actin primers, 5′-AGAGGGAAATCGTGCGTGAC-3′ and 5′-CAATAGTGATGACCTGGCCGT-3′; β-actin Taqman probe, FAM-CACTGCCGCATCCTCTTCCTCCCTAMRA-3′; IL-7 primers, 5′-CTGCAGTCCCAGTCATCATGA-3′ and 5′-GTGGCACTCAGATGATGTGACA-3′; IL-7 Taqman probe, FAM-CCTCCCGCAGACCATGTTCCATGT-TAMRA-3′; and *Foxp3* primers; 5′-GGCCCTTCTCCAGGACAGA-3′ and 5′-GCTGATCATGGCTGG GTTGT-3′; Foxp3 Taqman probe; FAM-ACTTCATGCATCAGCTCTCCACTGTGGAT-TAMRA. The conditions for real-time PCR were 94°C for 5 s and 60°C for 60 s for 40 cycles. The relative IL-6 and SOCS3 or IL-7 and foxp3 mRNA expressions were calculated as ratios to the HPRT or β-actin mRNA copy numbers.

We calculated the relative gene expression as follows; dividing the absolute copy number of target genes by the absolute copy number of housekeeping genes, such as HPRT or β-actin. We showed the raw data without normalizing them in figures of real-time PCR experiments.

Western blotting of IL-7 protein. The sLNs of irradiated type I-collagen-Cre/$STAT3^{flox/flox}$, wild type, or F759 were lysed with NP-40 cell lysis buffer (50 mM Tris-HCl, pH 8.0, 150 mM NaCl and 1% NP-40) containing protease inhibitors (Sigma-Aldrich). Protein fraction was purified by 2D Cleanup kit (BioRad Laboratories). After SDS page on a 10–20% gel, the protein fraction was applied on Western blotting analysis with anti–mouse IL-7 antibody (R&D Systems) plus horseradish peroxidase secondary antibody (Zymed Laboratories) and visualized by ECL (GE Healthcare).

Statistical analysis. All the data were statistically analyzed with a Student's *t* test.

Online supplemental material. Data regarding $CD25^+CD4^+$ T cells in F759 and N7Txed F759 mice is shown in Fig. S1, A–E, which is available at http://www.jem.org/cgi/content/full/jem.20052187/DC1.

We appreciate Ms. Iketani and Ms. Hayashi for their excellent technical assistance and thank Ms. Masuda and Ms. Kubota for their excellent secretarial assistance.

This work was supported by a Grant-in-Aid for Scientific Research from the Ministry of Education, Culture, Sports, Science and Technology in Japan; the Uehara Foundation; and the Osaka Foundation for the Promotion of Clinical Immunology.

The authors have no conflicting financial interests.

Submitted: 28 October 2005
Accepted: 21 April 2006

REFERENCES

1. Firestein, G.S. 2003. Evolving concepts of rheumatoid arthritis. *Nature.* 423:356–361.
2. Marrack, P., J. Kappler, and B. Kotzin. 2001. Autoimmune disease: why and where it occurs. *Nat. Med.* 7:899–905.
3. Hirano, T. 2002. Cytokines in autoimmune disease and chronic inflammatory proliferative disease. *Cytokine Growth Factor Rev.* 13:297–298.
4. Kontoyiannis, D., M. Pasparakis, T. Pizarro, F. Cominelli, and G. Kollias. 1999. Impaired on/off regulation of TNF biosynthesis in mice lacking TNF AU-rich elements: implications for joint and gut-associated immunopathologies. *Immunity.* 10:387–398.
5. Kollias, G., E. Douni, G. Kassiotis, and D. Kontoyiannis. 1999. The function of tumour necrosis factor and receptors in models of multiorgan inflammation, rheumatoid arthritis, multiple sclerosis and inflammatory bowel disease. *Ann. Rheum. Dis.* 58:I32–I39.
6. Hirano, T. 2002. Revival of the autoantibody model in rheumatoid arthritis. *Nat. Immunol.* 3:342–344.
7. Zenz, R., R. Eferl, L. Kenner, L. Florin, L. Hummerich, D. Mehic, H. Scheuch, P. Angel, E. Tschachler, and E. Wagner. 2005. Psoriasis-like skin disease and arthritis caused by inducible epidermal deletion of Jun proteins. *Nature.* 437:369–375.
8. Goldrath, A., and M. Bevan. 1999. Selecting and maintaining a diverse T-cell repertoire. *Nature.* 402:255–262.
9. Sprent, J., and C. Surh. 2002. T cell memory. *Annu. Rev. Immunol.* 20: 551–579.
10. Marrack, P., J. Bender, D. Hildeman, M. Jordan, T. Mitchell, M. Murakami, A. Sakamoto, B.C. Schaefer, B. Swanson, and J. Kappler. 2000. Homeostasis of αβ TCR^+ T cells. *Nat. Immunol.* 1:107–111.

11. Min, B., R. McHugh, G. Sempowski, C. Mackall, G. Foucras, and W. Paul. 2003. Neonates support lymphopenia-induced proliferation. *Immunity*. 18:131–140.
12. Tan, J.T., E. Dudl, E. LeRoy, R. Murray, J. Sprent, K.I. Weinberg, and C.D. Surh. 2001. IL-7 is critical for homeostatic proliferation and survival of naive T cells. *Proc. Natl. Acad. Sci. USA*. 98:8732–8737.
13. Clarke, S., and A. Rudensky. 2000. Survival and homeostatic proliferation of naive peripheral $CD4^+$ T cells in the absence of self peptide: MHC complexes. *J. Immunol*. 165:2458–2464.
14. Uehira, M., H. Matsuda, I. Hikita, T. Sakata, H. Fujiwara, and H. Nishimoto. 1993. The development of dermatitis infiltrated by γδ T cells in IL-7 transgenic mice. *Int. Immunol*. 5:1619–1627.
15. Watanabe, M., Y. Ueno, T. Yajima, S. Okamoto, T. Hayashi, M. Yamazaki, Y. Iwao, H. Ishii, S. Habu, M. Uehira, et al. 1998. Interleukin 7 transgenic mice develop chronic colitis with decreased interleukin 7 protein accumulation in the colonic mucosa. *J. Exp. Med*. 187: 389–402.
16. King, C., A. Ilic, K. Koelsch, and N. Sarvetnick. 2004. Homeostatic expansion of T cells during immune insufficiency generates autoimmunity. *Cell*. 117:265–277.
17. Hirano, T. 1998. Interleukin 6 and its receptor: ten years later. *Int. Rev. Immunol*. 16:249–284.
18. Hirano, T., T. Matsuda, M. Turne, N. Miyasaka, G. Buchan, B. Tang, K. Sato, M. Shimizu, R. Maini, M. Feldmann, et al. 1988. Excessive production of interleukin 6/B cell stimulatory factor-2 in rheumatoid arthritis. *Eur. J. Immunol*. 18:1797–1801.
19. Feldmann, M., F. Brennan, and R. Maini. 1996. Role of cytokines in rheumatoid arthritis. *Annu. Rev. Immunol*. 14:397–440.
20. Ishihara, K., and T. Hirano. 2002. IL-6 in autoimmune disease and chronic inflammatory proliferative disease. *Cytokine Growth Factor Rev*. 13:357–368.
21. Hata, H., N. Sakaguchi, H. Yoshitomi, Y. Iwakura, K. Sekikawa, Y. Azuma, C. Kanai, E. Moriizumi, T. Nomura, T. Nakamura, and S. Sakaguchi. 2004. Distinct contribution of IL-6, TNF-α, IL-1, and IL-10 to T cell-mediated spontaneous autoimmune arthritis in mice. *J. Clin. Invest*. 114:582–588.
22. Alonzi, T., E. Fattori, D. Lazzaro, P. Costa, L. Probert, G. Kollias, F. De Benedetti, V. Poli, and G. Ciliberto. 1998. Interleukin 6 is required for the development of collagen-induced arthritis. *J. Exp. Med*. 187:461–468.
23. Ohshima, S., Y. Saeki, T. Mima, M. Sasai, K. Nishioka, S. Nomura, M. Kopf, Y. Katada, T. Tanaka, M. Suemura, and T. Kishimoto. 1998. Interleukin 6 plays a key role in the development of antigen-induced arthritis. *Proc. Natl. Acad. Sci. USA*. 95:8222–8226.
24. Choy, E.H., D.A. Isenberg, T. Garrood, S. Farrow, Y. Ioannou, H. Bird, N. Cheung, B. Williams, B. Hazleman, R. Price, et al. 2002. Therapeutic benefit of blocking interleukin-6 activity with an anti-interleukin-6 receptor monoclonal antibody in rheumatoid arthritis: a randomized, double-blind, placebo-controlled, dose-escalation tria. *Arthritis Rheum*. 46:3143–3150.
25. Murakami, M., D. Kamimura, and T. Hirano. 2004. New IL-6 (gp130) family cytokine members, CLC/NNT1/BSF3 and IL-27. *Growth Factors*. 22:75–77.
26. Hirano, T., K. Nakajima, and M. Hibi. 1997. Signaling mechanisms through gp130: a model of the cytokine system. *Cytokine Growth Factor Rev*. 8:241–252.
27. Ohtani, T., K. Ishihara, T. Atsumi, K. Nishida, Y. Kaneko, T. Miyata, S. Itoh, M. Narimatsu, H. Maeda, T. Fukada, et al. 2000. Dissection of signaling cascades through gp130 in vivo: reciprocal roles for STAT3- and SHP2-mediated signals in immune responses. *Immunity*. 12:95–105.
28. Atsumi, T., K. Ishihara, D. Kamimura, H. Ikushima, T. Ohtani, S. Hirota, H. Kobayashi, S. Park, Y. Saeki, Y. Kitamura, and T. Hirano. 2002. A point mutation of Tyr-759 in interleukin 6 family cytokine receptor subunit gp130 causes autoimmune arthritis. *J. Exp. Med*. 196:979–990.
29. Ishihara, K., S. Sawa, H. Ikushima, S. Hirota, T. Atsumi, D. Kamimura, S. Park, M. Murakami, Y. Kitamura, Y. Iwakura, and T. Hirano. 2004. The point mutation of tyrosine 759 of the IL-6 family cytokine receptor gp130 synergizes with HTLV-1 pX in promoting rheumatoid arthritis-like arthritis. *Int. Immunol*. 16:455–465.
30. Asano, M., M. Toda, N. Sakaguchi, and S. Sakaguchi. 1996. Autoimmune disease as a consequence of developmental abnormality of a T cell subpopulation. *J. Exp. Med*. 184:387–396.
31. Goldrath, A., L. Bogatzki, and M. Bevan. 2000. Naive T cells transiently acquire a memory-like phenotype during homeostasis-driven proliferation. *J. Exp. Med*. 192:557–564.
32. Murakami, M., A. Sakamoto, J. Bender, J. Kappler, and P. Marrack. 2002. CD25+CD4+ T cells contribute to the control of memory CD8+ T cells. *Proc. Natl. Acad. Sci. USA*. 99:8832–8837.
33. Sakaguchi, S. 2004. Naturally arising $CD4^+$ regulatory T cells for immunologic self-tolerance and negative control of immune responses. *Annu. Rev. Immunol*. 22:531–562.
34. Pasare, C., and R. Medzhitov. 2003. Toll pathway-dependent blockade of $CD4^+CD25^+$ T cell-mediated suppression by dendritic cells. *Science*. 299:1033–1036.
35. Setoguchi, R., S. Hori, T. Takahashi, and S. Sakaguchi. 2005. Homeostatic maintenance of natural $Foxp3^+$ $CD25^+$ $CD4^+$ regulatory T cells by interleukin (IL)-2 and induction of autoimmune disease by IL-2 neutralization. *J. Exp. Med*. 201:723–735.
36. Al-Shami, A., R. Spolski, J. Kelly, T. Fry, P. Schwartzberg, A. Pandey, C. Mackall, and W. Leonard. 2004. A role for thymic stromal lymphopoietin in CD4(+) T cell development. *J. Exp. Med*. 200:159–168.
37. Sudo, T., M. Ito, Y. Ogawa, M. Iizuka, H. Kodama, T. Kunisada, S. Hayashi, M. Ogawa, K. Sakai, and S. Nishikawa. 1989. Interleukin 7 production and function in stromal cell–dependent B cell development. *J. Exp. Med*. 170:333–338.
38. Tyznik, A., J. Sun, and M. Bevan. 2004. The CD8 population in CD4-deficient mice is heavily contaminated with MHC class II–restricted T cells. *J. Exp. Med*. 199:559–565.
39. Yee, C.S., Y. Yao, P. Li, M.J. Klemsz, J.S. Blum, and C.H. Chang. 2004. Cathepsin E: a novel target for regulation by class II transactivator. *J. Immunol*. 172:5528–5534.
40. Wong, A.W., W.J. Brickey, D.J. Taxman, H.W. van Deventer, W. Reed, J.X. Gao, P. Zheng, Y. Liu, P. Li, J.S. Blum, et al. 2003. CIITA-regulated plexin-A1 affects T-cell-dendritic cell interactions. *Nat. Immunol*. 4:891–898.
41. Chang, C.H., and R.A. Flavell. 1995. Class II transactivator regulates the expression of multiple genes involved in antigen presentation. *J. Exp. Med*. 181:765–767.
42. Nozell, S., Z. Ma, C. Wilson, R. Shah, and E.N. Benveniste. 2004. Class II major histocompatibility complex transactivator (CIITA) inhibits matrix metalloproteinase-9 gene expression. *J. Biol. Chem*. 279: 38577–38589.
43. Xu, Y., L. Wang, G. Buttice, P.K. Sengupta, and B.D. Smith. 2004. Major histocompatibility class II transactivator (CIITA) mediates repression of collagen (COL1A2) transcription by interferon γ (IFN-γ). *J. Biol. Chem*. 279:41319–41332.
44. Ge, Q., D. Palliser, H. Eisen, and J. Chen. 2002. Homeostatic T cell proliferation in a T cell-dendritic cell coculture system. *Proc. Natl. Acad. Sci. USA*. 99:2983–2988.
45. Watanabe, N., S. Hanabuchi, V. Soumelis, W. Yuan, S. Ho, R. de Waal Malefyt, and Y. Liu. 2004. Human thymic stromal lymphopoietin promotes dendritic cell-mediated $CD4^+$ T cell homeostatic expansion. *Nat. Immunol*. 5:426–434.
46. Fry, T., M. Sinha, M. Milliron, Y. Chu, V. Kapoor, R. Gress, E. Thomas, and C. Mackall. 2004. Flt3 ligand enhances thymic-dependent and thymic-independent immune reconstitution. *Blood*. 104:2794–2800.
47. Mihara, M., Y. Moriya, T. Kishimoto, and Y. Ohsugi. 1995. Interleukin-6 (IL-6) induces the proliferation of synovial fibroblastic cells in the presence of soluble IL-6 receptor. *Br. J. Rheumatol*. 34:321–325.
48. Zhang, M., H. Tang, Z. Guo, H. An, X. Zhu, W. Song, J. Guo, X. Huang, T. Chen, J. Wang, and X. Cao. 2004. Splenic stroma drives mature dendritic cells to differentiate into regulatory dendritic cells. *Nat. Immunol*. 5:1124–1133.